CellPress

Glycolytic Shunts Replenish the Calvin–Benson–Bassham Cycle as Anaplerotic Reactions in Cyanobacteria

Alexander Makowka[1], Lars Nichelmann[1], Dennis Schulze[2], Katharina Spengler[1], Christoph Wittmann[2], Karl Forchhammer[3] and Kirstin Gutekunst[1,*]

[1]Department of Biology, Botanical Institute, University Kiel, 24118 Kiel, Germany

[2]Institute for Systems Biotechnology, Saarland University, 66123 Saarbrücken, Germany

[3]Organismic Interactions Department, Interfaculty Institute for Microbiology and Infection Medicine, University Tübingen, 72076 Tübingen, Germany

*Correspondence: Kirstin Gutekunst (kgutekunst@bot.uni-kiel.de)

https://doi.org/10.1016/j.molp.2020.02.002

ABSTRACT

The recent discovery of the Entner-Doudoroff (ED) pathway as a third glycolytic route beside Embden-Meyerhof-Parnas (EMP) and oxidative pentose phosphate (OPP) pathway in oxygenic photoautotrophs requires a revision of their central carbohydrate metabolism. In this study, unexpectedly, we observed that deletion of the ED pathway alone, and even more pronounced in combination with other glycolytic routes, diminished photoautotrophic growth in continuous light in the cyanobacterium *Synechocystis* sp. PCC 6803. Furthermore, we found that the ED pathway is required for optimal glycogen catabolism in parallel to an operating Calvin–Benson–Bassham (CBB) cycle. It is counter-intuitive that glycolytic routes, which are a reverse to the CBB cycle and do not provide any additional biosynthetic intermediates, are important under photoautotrophic conditions. However, observations on the ability to reactivate an arrested CBB cycle revealed that they form glycolytic shunts that tap the cellular carbohydrate reservoir to replenish the cycle. Taken together, our results suggest that the classical view of the CBB cycle as an autocatalytic, completely autonomous cycle that exclusively relies on its own enzymes and CO_2 fixation to regenerate ribulose-1,5-bisphosphate for Rubisco is an oversimplification. We propose that in common with other known autocatalytic cycles, the CBB cycle likewise relies on anaplerotic reactions to compensate for the depletion of intermediates, particularly in transition states and under fluctuating light conditions that are common in nature.

Key words: central carbohydrate metabolism, Calvin–Benson–Bassham cycle, Entner–Doudoroff pathway, oxidative pentose phosphate pathway, Embden–Meyerhof–Parnas pathway, cyanobacteria

INTRODUCTION

Autotrophic carbon fixation sustains life on Earth by providing cellular building blocks and a source of energy. Among the seven known CO_2 fixation pathways, the Calvin–Benson–Bassham (CBB) cycle is the most prominent one with the greatest contribution to global primary production (Fuchs, 2011; Overmann and Garcia-Pichel, 2013; Mall et al., 2018). It is utilized by many prokaryotes and all oxygenic photoautotrophs and has a comparably high demand of ATP (Bar-Even et al., 2012; Mall et al., 2018).

Cyanobacteria generate energy and reducing equivalents via the light reaction of photosynthesis. These are utilized to fix carbon in

the CBB cycle. The CBB cycle provides cells with carbohydrates for biosynthesis and storage (glycogen). Stored carbohydrates are obviously required to maintain metabolism in darkness (Saha et al., 2016). The breakdown of carbohydrates commences via three alternative glycolytic routes in cyanobacteria and plants: the Embden–Meyerhof–Parnas (EMP), the oxidative pentose phosphate (OPP), or the Entner–Doudoroff (ED) pathway (Chen et al., 2016). In cyanobacteria, even a fourth glycolytic route, the phosphoketolase (PK)

pathway, was identified (Alagesan et al., 2013; Xiong et al., 2015). Deletion of the OPP pathway in cyanobacteria results in mutants that are unable to grow under light-activated heterotrophic (LAH) conditions (Scanlan et al., 1995; Jansen et al., 2010). This is well in line with flux analyses that found that glucose is predominantly metabolized by the OPP pathway in darkness (Yang et al., 2002; Wan et al., 2017). It has furthermore been reported that the PK pathway in cyanobacteria contributes to heterotrophic metabolism as well (Xiong et al., 2015).

Aquatic habitats most commonly contain glucose as dissolved organic carbon (Lam and Simpson, 2008). This organic carbon originates predominantly from dead organic matter and serves as a basis for microbial metabolism (Alonso and Pernthaler, 2006; Klingner et al., 2015). Glucose concentrations vary and are especially high in coastal regions and during phytoplankton blooms (Ittekkot et al., 1981; Teeling et al., 2012). The presence of organic carbon in the light creates photomixotrophic conditions that allow cyanobacteria to fix CO_2 in parallel with glucose consumption (Gómez-Baena et al., 2008; Munoz-Marin et al., 2013; Chen et al., 2016). Anabolic (CBB cycle) and catabolic (glycolytic routes) processes thus operate simultaneously. The significance of photomixotrophy as a lifestyle in aquatic photoautotrophs has long been underestimated (Eiler, 2006; Hartmann et al., 2012; Moore, 2013). As a matter of principle, photoautotrophic metabolism, in which carbohydrates are synthesized from CO_2, runs in the opposite direction to heterotrophic metabolism, in which carbohydrates are broken down to CO_2. Obviously, the central carbon metabolism of photoautotrophs thus works in a bidirectional manner under photomixotrophic conditions. Flux analyses under photomixotrophic conditions in *Synechocystis* sp. PCC 6803 (hereafter referred to as *Synechocystis*) identified fluxes via the CBB cycle in parallel with fluxes via the OPP and EMP pathway (Yang et al., 2002; Nakajima et al., 2014). Glucose-6P was furthermore found to be isomerized by PGI (phosphoglucoisomerase) to fructose-6P, which directly entered the CBB cycle (Nakajima et al., 2014). The ED pathway was omitted in all these flux analyses as its presence was reported at a later time (Chen et al., 2016). Characterization of mutants, in which key enzymes of EMP, OPP, and ED pathway were deleted, revealed that growth under photomixotrophic conditions was retarded most severely in the absence of the ED pathway (Chen et al., 2016). Only sparse attention has been paid to the role of glycolytic pathways under photoautotrophic conditions, as they are intuitively regarded to be of minor importance in this context. A small flux through the OPP pathway was observed in *Synechocystis* under photoautotrophic conditions, which accounted for a loss of up to 13% of total fixed carbon via the decarboxylating reaction of 6P-gluconate dehydrogenase (Gnd) (Young et al., 2011; Matsuda et al., 2017). This futile cycling of CBB cycle and OPP pathway was proposed to routinely take place in plant chloroplasts as well (Sharkey and Weise, 2015). Its physiological role is not understood in detail, neither in cyanobacteria nor in plants. Even though the CBB cycle is regarded as an open cycle that participates in futile cycles in order to fine-tune metabolism, the CBB cycle is still illustrated in textbooks as being divided into three phases: (1) CO_2 fixation, (2) reduction of 3P glycerate to glyceraldehyde 3-phosphate (GAP), and (3) regeneration of the ribulose-1,5 BP (RuBP), from which the third regeneration phase is perceived to exclusively rely on

its own enzymes and CO_2 fixation. The perception of the CBB cycle is in this respect unusual and in contrast to other autocatalytic cycles such as, e.g., the tricarboxylic acid (TCA) cycle that is well known to depend on anaplerotic reactions for replenishment. The recent finding of an operating ED pathway in oxygenic photoautotrophs calls for a revision of their central carbon metabolism.

We found that glycolytic routes play a significant role under photoautotrophic growth conditions. They form anaplerotic shunts that replenish the CBB cycle by tapping cellular carbohydrate reservoirs in transition states and under fluctuating light conditions. Catabolic routes thus fine-tune CO_2 fixation under photoautotrophic conditions. This strengthens the view that bidirectionality is a strong principle in all biological processes and especially in the regulation of metabolism (Gutekunst, 2018).

RESULTS

Significance of Distinct Glycolytic Routes under Different Conditions

Glycolytic deletion mutants were grown under heterotrophic (LAH), fermentative, photomixotrophic, and photoautotrophic conditions. Our previous finding that deletion of the ED pathway (Δeda) had the strongest effect on the ability to grow under photomixotrophic conditions was confirmed (Figure 1B) (Chen et al., 2016). In darkness, i.e., under LAH and fermentative conditions, the OPP pathway (Δzwf, Δgnd) was most important (Figure 1C and 1D), which is well in line with previous findings (Scanlan et al., 1995; Yang et al., 2002; Jansen et al., 2010; Wan et al., 2017). Deletion of the EMP pathway (Δpfk) led to diminished growth under LAH conditions but the effect was less severe than in Δzwf and Δgnd. Under fermentative conditions, Δpfk recovered like the wild type (WT). Deletion of the ED pathway (Δeda) had no effect in darkness, under neither LAH nor fermentative conditions (Figure 1C and 1D).

It must be noted that under fermentative conditions strains were tested for their ability to survive rather than grow, as cells hardly divide in this setting. For this purpose, cultures were kept for 7 days under dark, anoxic conditions and brought to continuous light thereafter to monitor their ability to resume growth (Figure 1D). During recovery, external glucose concentrations declined at a similar rate as growth resumed (Supplemental Figure 1). Under photoautotrophic conditions, Δeda and Δzwf grew at rates slightly below that of the WT (Figure 1A).

Glycolytic Routes under Photoautotrophic Growth

Under photoautotrophic conditions, the differences in growth between WT and glycolytic deletion strains seemed minor at first sight (Figure 1A). However, as the growth of Δeda was typically slightly diminished in comparison with the WT (Figure 1A), data of 18 independent growth experiments (each containing three replicates) were analyzed in depth. To simplify and standardize comparison of growth curves of different experiments, we developed a novel growth evaluation method based on a triplet regression model, which gives out growth rates in comparison with the WT (Supplemental Text 1, Supplemental Figures 2 and 3, and Supplemental Tables 1 and 2). Indeed, Δeda showed a significant growth impairment of 18% in comparison with the
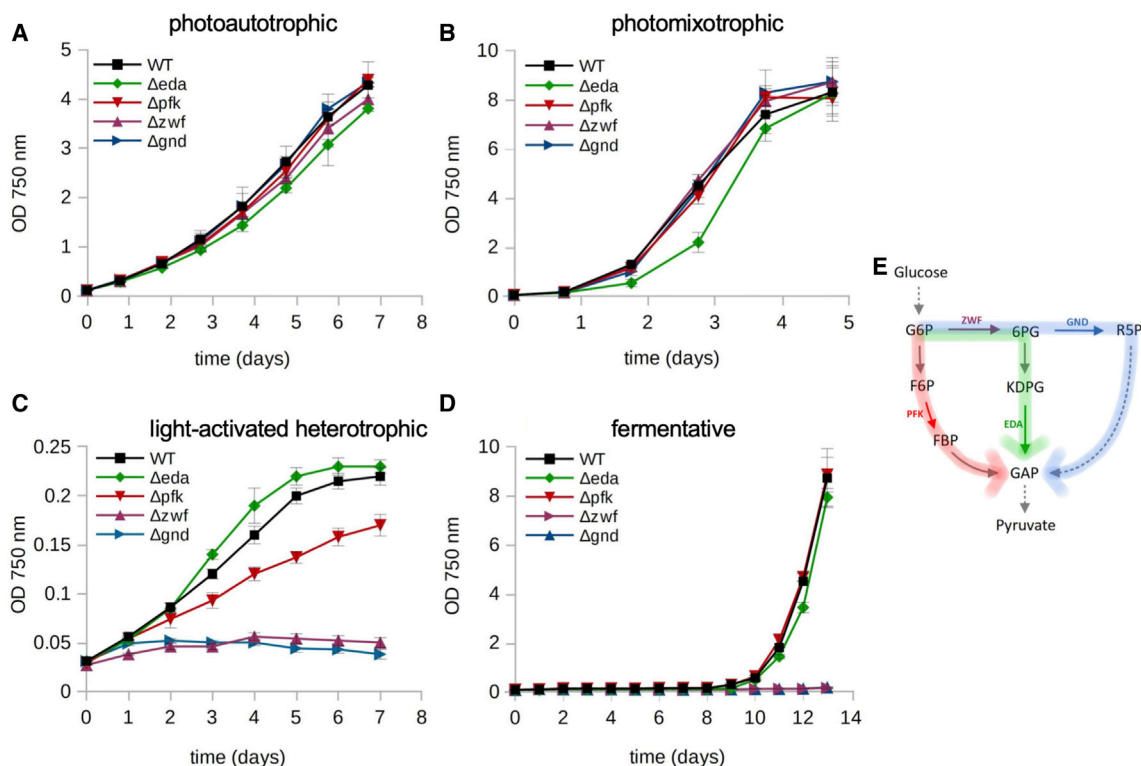
Figure 1. Growth of Glycolytic Deletion Mutants under Different Growth Conditions.

(A–D) Growth of WT, Δeda, Δpfk, Δzwf, and Δgnd under **(A)** photoautotrophic, **(B)** photomixotrophic, **(C)** light-activated heterotrophic, and **(D)** fermentative conditions.

(E) Simplified scheme of glycolytic routes (Embden–Meyerhof–Parnas [EMP], red; oxidative pentose phosphate [OPP], blue; Entner–Doudoroff [ED], green).

WT (p = 0.002), with a relative growth rate of 0.82 under photoautotrophic conditions (Figure 2A).

For Δgnd and Δpfk, no differences in growth behavior were observed in comparison with the WT. By contrast, Δzwf also displayed an impaired growth rate compared with the WT (−18%, p = 0.163); however, the results remain uncertain due to the small sample size (n = 5). Glycolytic eda double mutants showed even more pronounced growth impairments: ΔedaΔpfk (−37%, p = 0.023), ΔedaΔzwf (−42%, p < 0.001), and ΔedaΔgnd (−60%, p < 0.001) (Figure 2A and 2B). We hypothesized that 6P-gluconate (6PG) might accumulate in ΔedaΔgnd, as the interruption of OPP and ED pathway might hinder its conversion (see also Figure 4). 6P-gluconate is known to bind to the active site of Rubisco as an activator at low concentrations but acts as competitive inhibitor against the substrate RuBP at higher concentrations (Badger and Lorimer, 1981; Matsumura et al., 2012). Artificially high concentrations of 6P-gluconate could thus be responsible for the tremendous growth impairment in ΔedaΔgnd. In fact, 6P-gluconate accumulated in ΔedaΔgnd but was below detection levels in WT and all other glycolytic mutants (Figure 2D). In line with these results, CO_2 fixation was severely reduced in ΔedaΔgnd in comparison with the WT and all other glycolytic mutants (Figure 2E). Fluxes through the ED pathway were shown to be negligible under heterotrophic and photomixotrophic conditions in *Synechocystis* (Wan et al., 2017), whereas photoautotrophic conditions were not tested. A requirement for classical flux analyses are constant conditions that result in

metabolic steady states. This requirement obviously creates a somewhat artificial situation that, however, allows a snapshot of metabolic fluxes under these confined conditions. Our cultures were grown in glass tubes with a diameter of 3.5 cm, illuminated from two sides. Relative light-intensity distributions in the cultures depending on optical density were determined with an illuminator and revealed highly heterogeneous light regimes, especially with increasing optical density due to mutual shading of cells that naturally increases to the center of the tubes (Supplemental Figure 4A). As the cultures were continuously mixed by constant flushing, single cells that were swirled through the tubes thus in actual fact encountered fluctuating light conditions even under constant illumination. As no metabolic steady state was reached under these conditions, the requirements for classical quantitative flux analyses were not met. Therefore, WT and ΔedaΔgnd were cultivated additionally in shaking flasks with more homogeneous light-intensity distributions (Supplemental Figure 4B). The growth impairment of ΔedaΔgnd persisted under these conditions (Supplemental Figure 4C). However, 6P-gluconate contents of WT and ΔedaΔgnd were similar in contrast to cultivation in glass tubes with heterogeneous light intensities (compare Figure 2D and Supplemental Figure 4D). Even if only minor fluxes via ED and OPP pathways occur via Eda and Gnd, a higher accumulation of 6P-gluconate in the deletion mutant can be expected, in contrast to the WT. Our results thus indicate that this flux might well exist in heterogeneous light (Figure 2D) but is absent under metabolic steady state in homogeneous light (Supplemental Figure 4D). The growth impairment of ΔedaΔgnd
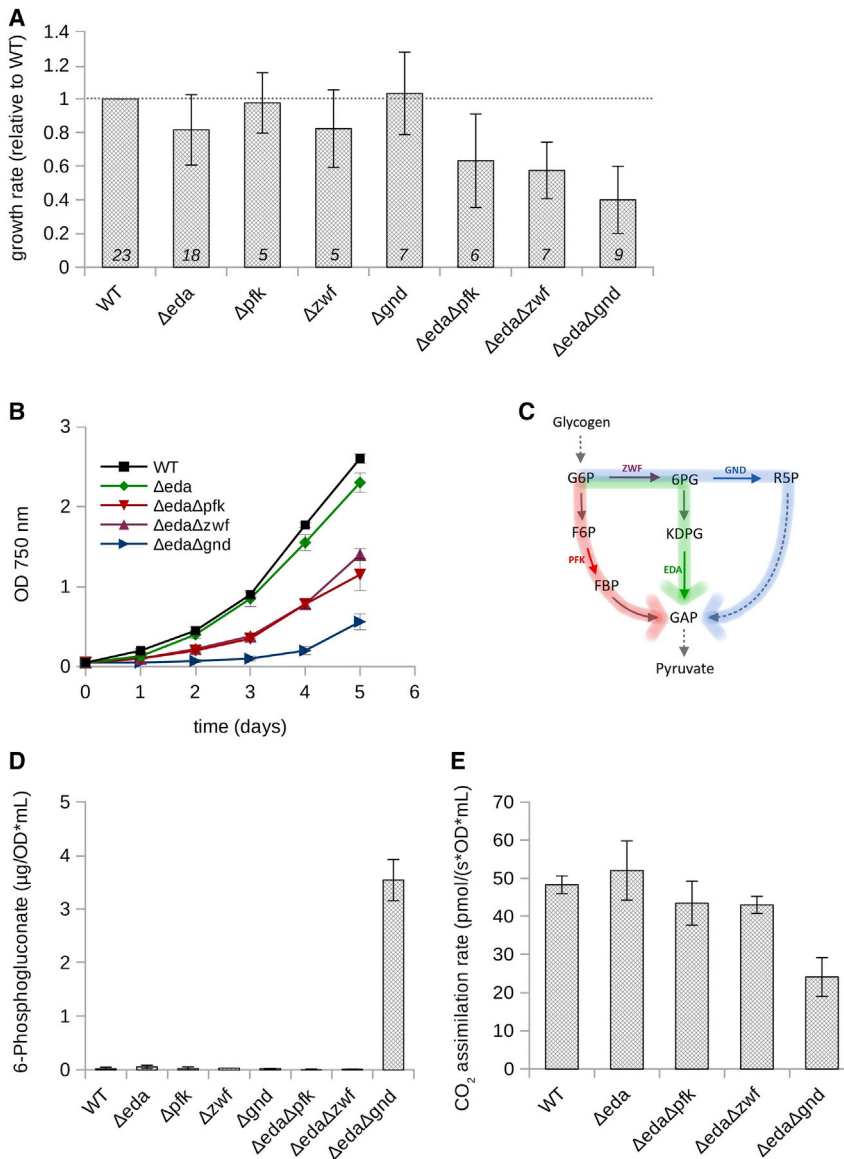
Figure 2. Growth Behavior, Cellular 6P-Gluconate Contents and CO_2 Assimilation Rates of WT and Various Mutants under Photoautotrophic Conditions.

(A) Mean growth rates in comparison with WT. Values inside bars represent number of independent experimental repetitions (n).

(B) Traces of photoautotrophic growth experiments.

(C) Simplified scheme of glycolytic routes (EMP, red; OPP, blue; ED, green).

(D) Cellular 6P-gluconate contents of WT, Δeda, Δpfk, Δzwf, Δgnd, ΔedaΔpfk ΔedaΔzwf, and ΔedaΔgnd under photoautotrophic conditions.

(E) CO_2 assimilation rate of WT, Δeda, ΔedaΔpfk, ΔedaΔzwf, and ΔedaΔgnd under photoautotrophic conditions.

and WT under photoautotrophic conditions. No differences were observed between Δpfk, Δzwf, Δgnd, and WT, whereas Δeda had significantly increased glycogen content (+145%, $p < 0.001$) under these conditions (Figure 3A). One should note that all data in this study are shown relative to OD_{750} values, as Δeda contains significantly less chlorophyll compared with the WT (Supplemental Figure 5).

The ED pathway is special among the glycolytic routes as it does not share any reactions and intermediates with the CBB cycle. This diminishes the risk of mutual inhibition (Figure 4) (Chen et al., 2016). We therefore hypothesized that glycogen breakdown might be decelerated particularly in the absence of the ED pathway under photoautotrophic conditions when the cells fix CO_2 via the CBB cycle. WT, Δeda, Δpfk, Δzwf, and Δgnd were transferred from photomixotrophic conditions, in which cells accumulate high amounts of glycogen, to either photoautotrophic or LAH conditions for the purpose of comparing the rates of glycogen consumption during this transfer between mutants either in the presence (light) or absence (darkness) of an active CBB cycle (Figure 3C–3G). Deletion of the EMP pathway (Δpfk) had hardly any effect on glycogen degradation rates in light and darkness (Figure 3E). In the absence of the OPP pathway (Δzwf, Δgnd), glycogen consumption was severely reduced under LAH conditions, whereas glycogen consumption occurred at WT levels in the light (Figure 3F and 3G). Deletion of the ED pathway (Δeda) led to a minor reduction in glycogen consumption rates in darkness. However, in striking contrast, under photoautotrophic conditions in the light the glycogen consumption rate was strongly reduced in Δeda in comparison with the WT, as expected (Figure 3C, 3D, 3H, and 3I). This is well in line with the assumption that the ED pathway is especially beneficial for cells in the presence of an active CBB cycle. However, the measured net glycogen consumption rates are a result of glycogen synthesis and degradation. As both the glycogen content and the measured net

in homogeneous light might thus as well result from potential moonlight functions of Eda and Gnd. Furthermore, as the concentrations of 6P-gluconate in WT and ΔedaΔgnd grown in homogeneous light lay only slightly below the levels determined for ΔedaΔgnd cultivated in heterogeneous light, it is unlikely that an inhibitory effect of the metabolite alone is responsible for diminished CO_2 fixation. The phenotype of ΔedaΔgnd cannot thus be explained satisfactorily at this point but requires further studies. Our results furthermore emphasize that the absence of substantial fluxes through pathways under metabolic steady state should not lead to the conclusion that a pathway is of minor importance under natural conditions.

The Entner–Doudoroff Pathway Allows Optimal Glycogen Degradation in the Presence of an Operating Calvin–Benson–Bassham Cycle in the Light

As glycogen provides the substrate for all glycolytic routes, its cellular concentration was analyzed in Δeda, Δpfk, Δzwf, Δgnd,
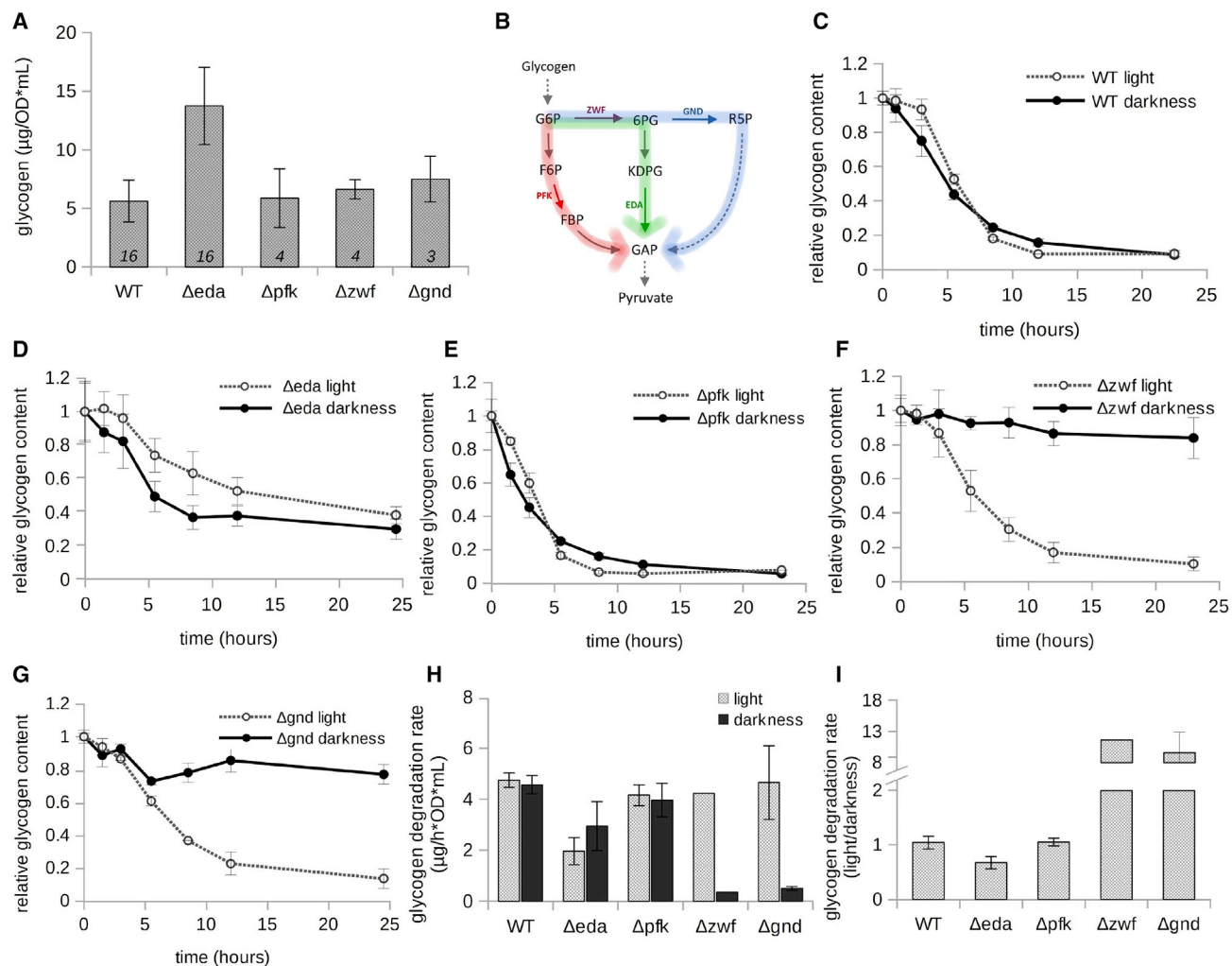
Figure 3. Cellular Glycogen Contents under Photoautotrophic Conditions and Glycogen Degradation Rates of Various Glycolytic Deletion Mutants after Transfer from Photomixotrophic to either Photoautotrophic or Heterotrophic Conditions.

(A) Mean cellular glycogen contents of WT, Δeda, Δpfk, Δzwf, and Δgnd.
(B) Simplified scheme of glycolytic routes (EMP, red; OPP, blue; ED, green).
(C–G) Cellular glycogen contents of WT (C), Δeda (D), Δpfk (E), Δzwf (F), and Δgnd (G).
(H) Glycogen degradation rates of WT, Δeda, Δpfk, Δzwf, and Δgnd.
(I) Glycogen degradation rate in the light compared with glycogen degradation rate in darkness in WT, Δeda, Δpfk, Δzwf, and Δgnd.

glycogen consumption rate of Δzwf in the light was similar to that of the WT and as deletion of zwf should interrupt the ED pathway, it might well be the case that the enhanced glycogen content of Δeda as well as its reduced net glycogen consumption rate in the light is actually a result of faster glycogen synthesis.

Suggested Rationale behind the Significance of Glycolytic Routes under Photoautotrophic Conditions

Under photoautotrophic conditions, *Synechocystis* fixes CO_2 via the CBB cycle, which yields carbohydrates for storage purposes (glycogen) and intermediates for biosynthesis. Photosynthesis furthermore provides ATP and reducing equivalents. A role of glycolytic routes under these conditions is thus at first sight counterintuitive. They are obviously required for neither the supply of ATP, reducing equivalents, nor biosynthetic intermediates. Furthermore, glycolytic routes operate as a matter of principle

in the opposite direction to the CBB cycle. This bears the risk of mutual inhibition, as several enzymes and intermediates are shared by these opposing processes. The dimension of overlap between glycolytic pathways and CBB cycle is visualized in Figure 4A–4C.

This great extent of shared reactions and intermediates is challenging, especially in prokaryotes that lack subcellular compartmentation. Obviously, if CO_2 fixation is operating, the CBB cycle counteracts to the EMP pathway at the level of fructose-6P, whereas the OPP pathway and CBB cycle collide at the level of ribulose-5P. The ED pathway is exceptional in the sense that it does not overlap with the CBB cycle (Figure 4C). Based on the scheme shown in Figure 4, we hypothesized that glycolytic routes might not operate at their full length from glycogen to pyruvate (with the exception of the ED pathway) under photoautotrophic conditions but might instead form glycolytic
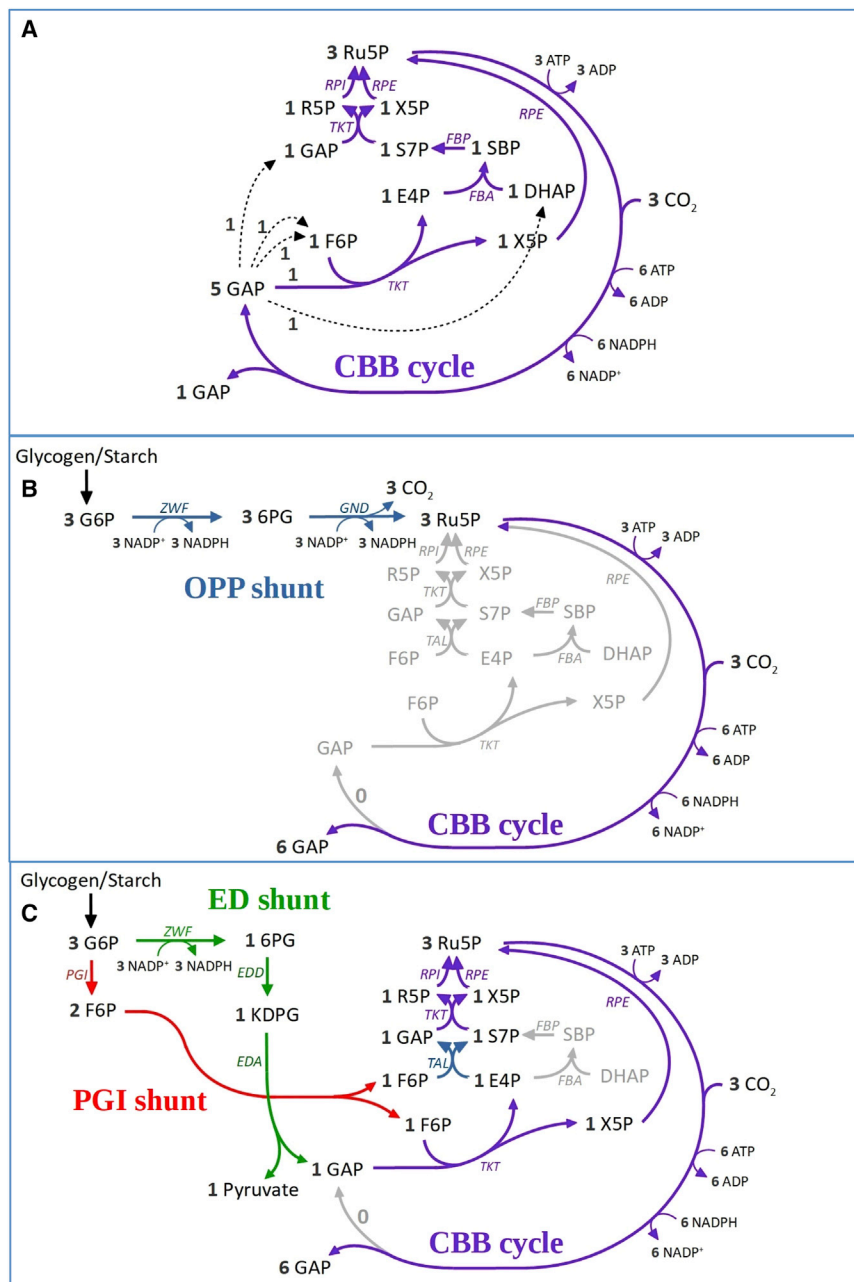
Figure 4. Overlap between the Glycolytic Pathways and CBB Cycle.

(A) Calvin–Benson–Bassham (CBB) cycle in purple.

(B) Glycolytic routes: Emden–Meyerhof–Parnas (EMP) pathway in red, Entner–Doudoroff (ED) pathway in green, oxidative pentose phosphate (OPP) pathway in blue. Lower glycolysis is shown in black.

(C) An overlay of CBB cycle and glycolytic routes reveals the dimension of overlapping reactions. As CBB cycle and glycolytic routes operate in opposite directions, overlaps highlight reactions with a high risk for mutual inhibition. We propose that glycolytic routes are reduced to glycolytic shunts (OPP shunt in blue, PGI shunt in red, ED shunt in green) in the presence of an active CBB cycle.

called glucose-6P shunt) back into the cycle (Sharkey and Weise, 2015). This glucose-6P shunt is identical to the proposed OPP shunt. The shunt is supposed to form a futile cycle with the CBB cycle, which consumes ATP, does not result in CO_2 fixation (as Gnd catalyzes a decarboxylating reaction, which annuls the carboxylating reaction of Rubisco), and leaves the NADPH level unchanged. It has thus been suggested that this futile cycle is a means to fine-tune and stabilize photosynthesis (Sharkey and Weise, 2015). We would like to expand this view. Even though the CBB cycle is perceived as open, it is commonly taught in classes that the regeneration phase of the CBB cycle relies exclusively on its own enzymes and that this autocatalytic cycle thus works completely autonomously (Figure 5A). According to the classical view, three rounds of CO_2 fixation result in three molecules of RuBP (each C5) that are converted to three 6-carbon intermediates, which spontaneously fragment into six triosephosphates (each C3). Five of these triosephosphates are required to regenerate three molecules of RuBP, whereas one molecule triosephosphate can be drained off the CBB cycle. Admittedly, the situation might be rather simple when triosephosphates are required for biomass synthesis. However, regeneration of RuBP is stoichiometrically more challenging if riboses for nucleotide synthesis or erythrose-4P for amino acid synthesis are required and drained off the cycle. In particular, changing environmental conditions such as fluctuating light may require a higher flexibility from the CBB cycle than is provided by regeneration via the well-described CBB cycle route. An autocatalytic cycle such as the CBB cycle can only operate if a depletion of its intermediates is successfully avoided (Barenholz et al., 2017). Two alternative replenishing pathways can be imagined (Figure 5B and 5C; Supplemental Text 2): (1) OPP

shunts that replenish the CBB cycle upon demand and are thus part of its regenerative phase. These bypasses were named PGI shunt, OPP shunt, and ED shunt. The name EMP shunt was omitted, as Pfk, which is the key enzyme of the EMP pathway, should not be part of the shunt according to the scheme.

In plants it has been proposed that a constant flow of carbon might exist as a bypass reaction of the CBB cycle via Zwf and Gnd (the so-

Figure 5. Classical and Updated Views about the Regeneration of Ribulose-5P in the CBB Cycle, Including the Roles of Glycolytic Shunts.

(A) Classical view of the CBB cycle as an exclusively autonomously operating autocatalytic cycle. One molecule of triosephosphate (GAP) can be drained off for biosynthesis every third round of CO_2 fixation, whereas five molecules of triosephosphates (GAPs) are required for regeneration of three molecules of ribulose-5P (Ru5P).

(B) Regeneration of Ru5P via the OPP shunt: three molecules of glucose-6P (G6P) are decarboxylated via the OPP shunt to yield three molecules of Ru5P plus three CO_2.

(C) Regeneration of Ru5P via a combination of PGI and ED shunt: two molecules of G6P enter the PGI shunt and one molecule of G6P enters the ED shunt to yield two molecules of fructose-6P (F6P) and one triosephosphate (GAP) that are further converted to yield three molecules of Ru5P and one molecule of pyruvate. Glucose-6P (G6P) originates from the CBB cycle or alternatively from the glycogen reservoir.

stronger flux through the OPP shunt (accompanied by CO_2 loss) to replenish the CBB cycle. In this sense, we cannot ascertain at this point whether the growth phenotype of Δ*eda* is caused by the missing flux through the ED pathway or rather results from redirected fluxes and/or the accumulation of intermediates that were induced by the deletion of *eda*. In addition, we obviously cannot rule out that Eda has a moonlight function.

Glycolytic Shunts Support Activation of the Calvin–Benson–Bassham Cycle

With the purpose of testing the hypothesis that PGI, OPP, and ED shunts replenish the CBB cycle and are thus part of its regenerative phase, we first tried to delete *pgi* but were not successful as we merely obtained a merodiploid mutant (*pgi*Δ*pgi*) that kept high enzymatic activities of Pgi and it was thus not impaired in its growth (Supplemental Figure 6A and 6B). In a second approach we kept Δ*eda*, Δ*pfk*, Δ*zwf*, Δ*gnd*, and WT for 5 min in darkness to arrest the CBB cycle with the aim of monitoring its reactivation upon illumination in relation to the glycolytic shunts (Figure 6).

The light reaction of photosynthesis commences immediately upon illumination whereas reactivation of the CBB cycle is typically delayed (Howard et al., 2008; Papageorgiou et al., 2007; Tamoi et al., 2005). Upon illumination, photochemical quenching (q_P) at photosystem II (PSII) was measured in the absence of nitrate (which is an effective electron sink of the photosynthetic electron chain) and oxygen (which is an effective electron acceptor via the Mehler-like reaction at
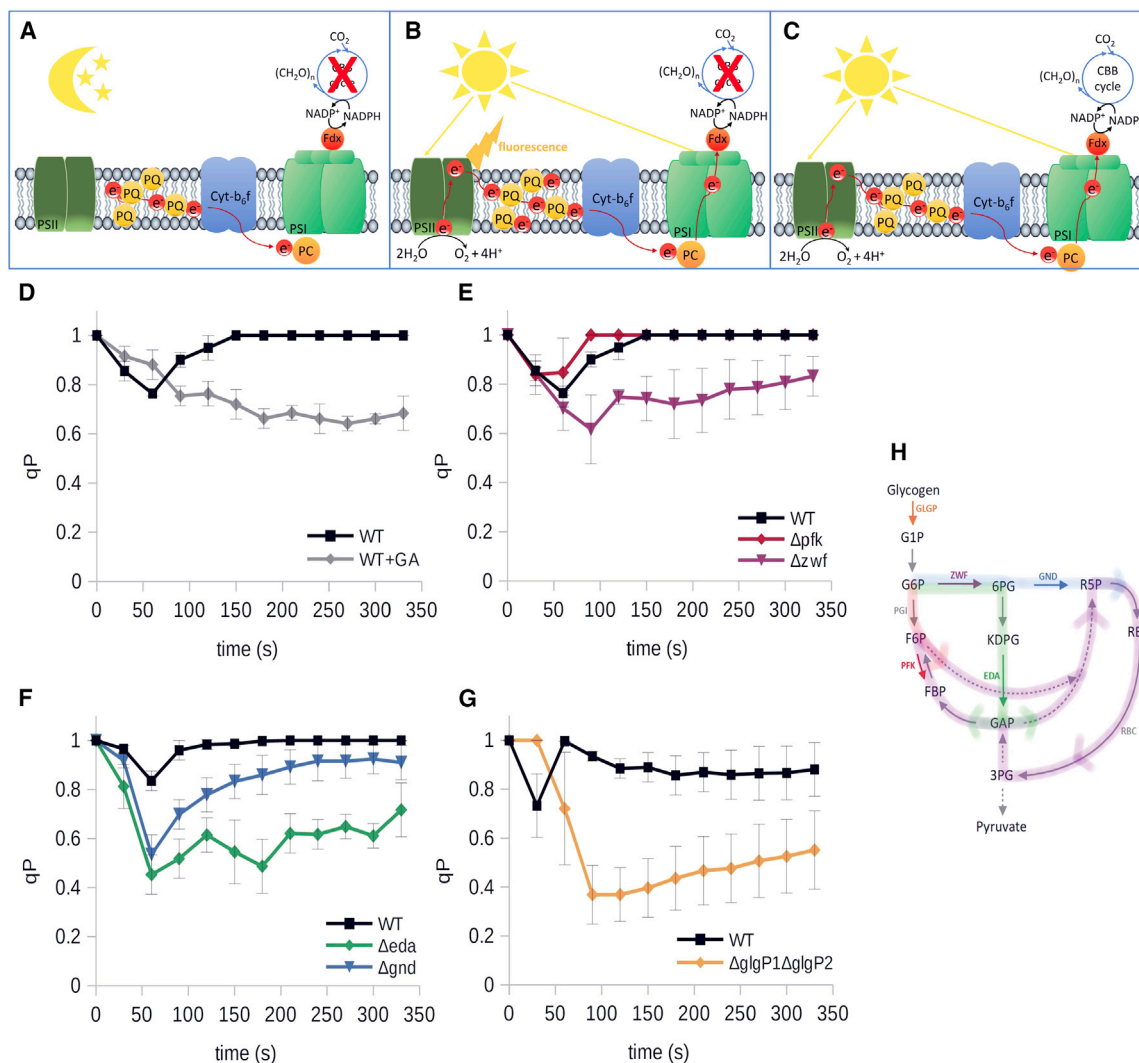
Shunt. Ribulose-5P could be provided via Zwf and Gnd from glucose-6P descending from the CBB cycle and/or alternatively from the cellular carbohydrate reservoir (Figure 5B), and (2) PGI Shunt and ED Shunt. Alternatively, two molecules of fructose-6P (each C6) provided either by the CBB cycle or again via a shunt from glycogen via Pgi could be combined with one GAP (C3) from the ED pathway to allow the regeneration of three ribulose-5P (each C5) (Figure 5C).

It should be noted that replenishing the CBB cycle via the OPP shunt (Figure 5B) results in higher carbon loss compared with the classical pathways (Figure 5A) or a combination of PGI and ED shunt (Figure 5C). This is due to the decarboxylating reaction catalyzed by Gnd. The poorer growth of Δ*eda* under photoautotrophic conditions might thus in fact be a result of a

Figure 6. Photochemical Fluorescence Quenching at Photosystem II upon Illumination of Dark-Adapted Cells via the Activation of the Calvin–Benson–Bassham Cycle Related to Glycolytic Shunts and Glycogen Catabolism.

(A–C) Experimental setup, **(D–G)** photochemical fluorescence quenching (q_P) measurements, and **(H)** simplified scheme of glycolytic shunts (PGI shunt, red; OPP shunt, blue; ED shunt, green; CBB cycle, purple).

(A) In darkness neither the photosynthetic electron chain nor the CBB cycle operate.

(B) Upon illumination PSII and PSI are immediately excited, whereas the CBB cycle is only activated with a delay. This results in a backlog of electrons that causes fluorescence at PSII.

(C) The fluorescence is quenched photochemically () as soon as the CBB cycle accepts electrons from the photosynthetic electron chain. Increase of photochemical fluorescence quenching (q_P) is thus a direct readout of the reactivation of the CBB cycle.

(D) As a validity check and control, glycolaldehyde (GA) was added to the assays, which inhibited the CBB cycle and blocked the observed increase in photochemical fluorescence quenching (q_P) in the WT.

(D–G) Photochemical fluorescence quenching (q_P) in WT, various glycolytic mutants (Δpfk, Δzwf, Δgnd, Δeda), and $\Delta glgP1\Delta glgP2$, which is unable to catabolize glycogen.

photosystem I [PSI]). At the onset of light, fluorescence quenching at PSII was low due to the incapacity of the photosystem to dispose of electrons into the photosynthetic chain (Figure 6). Subsequently, PSII fluorescence quenching was increased by the onset of the CBB cycle, which accepts electrons from the photosynthetic chain. To validate this approach, we applied glycolaldehyde (GA), which specifically inhibits the CBB cycle via inhibition of phosphoribulokinase (Sicher, 1984; Stokes and Walker, 1972). Increase of photochemical fluorescence quenching () was completely absent in the presence of GA,

which confirms that the CBB cycle is indeed responsible for the observed quenching (Figure 6D). The described setting thus allowed us to observe the activation of the CBB cycle after its arrest by dark incubation. We also monitored PSII and PSI activities in WT and mutant strains as a control. PSII and PSI activity measurements under physiological growth conditions did not reveal any significant differences between the WT and mutants (Δeda, Δgnd, Δpfk, Δzwf, and $\Delta glgP1\Delta glgP2$) (Supplemental Figure 9), which indicates that q_P measurements provide comparable data in WT and mutant strains. It was

furthermore ascertained that state transition—modifications in the preference of transfer of excitation energy from the phycobilisomes to either PSII and PSI—was not responsible for the observed changes in photochemical quenching (Supplemental Figure 10). As Pfk is not part of the PGI shunt, we hypothesized that Δpfk would be unaffected in its ability to reactivate the CBB cycle after dark arrest. As expected, deletion of the EMP pathway (Δpfk) had no effect (Figure 6E). However, deletion of either OPP (Δzwf, Δgnd) or ED (Δeda) shunt delayed the onset of the CBB cycle significantly (Figure 6E and 6F). To check further whether the glycolytic shunts tap the soluble glucose-6P pool or alternatively resort to the glycogen reservoir to replenish the CBB cycle, we generated a double mutant ($\Delta glgP1\Delta glgP2$) in which both isoforms of glycogen phosphorylase ($glgP1$ and $glgP2$) were deleted. It was shown previously that $\Delta glgP1\Delta glgP2$ is unable to catabolize glycogen (Doello et al., 2018). Inhibition of glycogen breakdown delayed the activation of the CBB cycle (Figure 6G). This reveals that glycolytic shunts indeed utilize storage carbohydrates to replenish the CBB cycle upon demand. We thus propose that OPP, PGI, and ED shunts constitute an anaplerotic network for the CBB cycle under photoautotrophic conditions, which commences with glycogen. We furthermore suggest that glycolytic shunts are part of two distinct networks that depend on the origin of the catabolized glucose-6P. Scenario 1 (anaplerotic network): In the case that glucose-6P originates from glycogen, all three mentioned glycolytic shunts form classical anaplerotic reactions. This is important at dark–light transitions to start the CBB cycle and in situations when intense consumption of CBB cycle intermediates endangers the regeneration of ribose-5P. Scenario 2 (regulatory network): In the case that glucose-6P originates directly from the CBB cycle, obviously the PGI shunt should not be of importance due to mutual inhibition. However, stoichiometric calculations reveal that the utilization of either OPP or ED shunt distinctly influences cellular ATP/NADPH levels and the CO_2-fixation efficiency of the CBB cycle and have thus the potential to form a regulatory network to fine-tune photosynthesis, as proposed earlier for the OPP shunt (Supplemental Text 2, Supplemental Figures 7 and 8, and Supplemental Tables 3 and 4) (Sharkey and Weise, 2015).

DISCUSSION

Photoautotrophic fluxes via Zwf and Gnd into the CBB cycle have been observed in both cyanobacteria and plants (Young et al., 2011; Sharkey and Weise, 2015; Matsuda et al., 2017). These fluxes were interpreted to result from incomplete downregulation of both enzymes in the light, accompanied by undesired carbon loss and a reduction in photosynthetic efficiency (Young et al., 2011). It was furthermore suggested that Zwf and Gnd form a futile cycle with the CBB cycle to stabilize photosynthesis (Sharkey and Weise, 2015; Matsuda et al., 2017). A flux via the described PGI shunt into the CBB cycle has been reported under photomixotrophic conditions (Nakajima et al., 2014). In an engineered strain of *Synechococcus elongates* PCC 7942, overexpression of either Pgi or a combination of Zwf and Gnd resulted in higher growth rates under photomixotrophic conditions (Kanno et al., 2017). Furthermore, when CP12, which might repress the CBB cycle under photomixotrophic conditions, was deleted in the *zwf/gnd* overexpression strain, the substrate of Rubisco that accumulated in the presence of glucose and

CO_2 fixation was enhanced, which indicates that a flux via Zwf and Gnd supplied the CBB cycle with intermediates (Kanno et al., 2017). We suggest that this admittedly highly artificial flux in an engineered *Synechococcus* strain under photomixotrophic conditions might indeed also exist in a similar manner routinely under photoautotrophic conditions. Autocatalytic cycles such as the CBB or TCA cycle require stable fluxes (Barenholz et al., 2017). Hence, they need to avoid both depletion and accumulation of intermediates by balancing anaplerotic and cataplerotic reactions (Owen et al., 2002). In this sense, it was shown in *Escherichia coli* that non-native CO_2 fixation via an introduced CBB cycle (by addition of PRK and Rubisco to the existing OPP pathway in *E. coli*) was only successful upon modification of enzymes that catalyze reactions at branch points to biomass synthesis and was thus allowed to balance fluxes (Antonovsky et al., 2016). Whereas the TCA cycle has long since been known to be an autocatalytic cycle that depends on anaplerotic reactions, the CBB cycle is regarded as a self-sufficient completely autonomous route that exclusively relies on CO_2 fixation and its own enzymes to avoid depletion of its intermediates. However, our results indicate that this is an oversimplification and misconception. Instead, the CBB cycle operates in a manner similar to that of the TCA cycle, regulated by a network of replenishing and consuming reactions that secure its continuous operation.

A glycolytic route that has been neglected in this study is the phosphoketolase (PK) pathway, which was recently discovered in cyanobacteria (Xiong et al., 2015). The key enzyme of this pathway is phosphoketolase (XFP), which is a generalist enzyme with the potential to either cleave xylulose-5P, fructose-6P, or seduheptulose-7P to acetyl-P and the corresponding aldose phosphate (Krüsemann et al., 2018). *Synechocystis* possesses two XFP isoenzymes (*slr0432* and *sll0529*) that have not been characterized biochemically so far in this organism. It is, however, unlikely that it forms an additional glycolytic shunt to replenish the CBB cycle, as it is identical to the OPP pathway in its first reactions and branches off this pathway (or alternatively the CBB cycle) for the supply of acetyl-P (Supplemental Figure 11A–11E). Investigations that are required to clarify this task are ongoing. The PK pathway has so far not been described in plants, in contrast to the EMP, OPP, and ED pathways.

The existence of anaplerotic glycolytic shunts that are connected to the CBB cycle might furthermore explain why plant chloroplasts possess key enzymes of glycolytic pathways but often lack enzymes belonging to lower glycolysis, which are not part of the described shunts (Facchinelli and Weber, 2011; Flügge et al., 2011). Glycolytic routes thus fulfill a dual function in cyanobacteria: they operate in their full length to catabolize stored carbohydrates at night and form shunts to replenish the CBB cycle during the day, especially in transition states and under fluctuating light conditions that are common in nature. The CBB cycle thus builds up its own carbohydrate reservoir that can be tapped on demand for fine-tuning and anaplerosis.

METHODS

Growth Conditions

For growth experiments, *Synechocystis* sp. PCC 6803 WT and mutants of this strain (Supplemental Table 6) were grown in 250 ml of BG11 medium

(pH 8) at 28°C in glass tubes with a diameter of 3.5 cm that were illuminated from two sides under constant light (50 μmol m^{-2} s^{-1}). Cultures were aerated with filter-sterilized air. For one experiment (Supplemental Figure 4), WT and $\Delta eda\Delta gnd$ were alternatively cultivated under photoautotrophic conditions in 250 ml of baffled shake flasks equipped with translucent caps, filled with 25 ml of medium, and incubated on a rotary shaker (28°C, 50 μE m^2 s^{-1}, 100 rpm; Infors Multitron; Infors, Basel, Switzerland). Photomixotrophic, LAH, and fermentative cultures were supplemented with 10 mM glucose. Photomixotrophic cultures were kept under constant illumination. Heterotrophic (LAH) and fermentative cultures were kept in darkness and illuminated for 10 min every 24 h. LAH cultures were aerated, fermentative cultures were purged for 5 min with N$_2$ with the purpose of creating anoxic conditions and subsequently kept without aeration. As cells do not grow under fermentative conditions, cultures were brought back to light on day 7 in order to monitor their ability to resume growth. As we were most interested in the ability of the strains to utilize CO$_2$ and glycogen to build up biomass, we decided that cellular dry weight would be most interesting. Determining cellular dry weights on a daily basis is, however, very time consuming. We therefore measured OD$_{750}$ and cellular dry weight and found a very good correlation for both the WT and Δeda (Supplemental Figure 12). OD$_{750}$ was thus monitored on a daily basis.

Generation of Deletion Mutants

Constructs for deletion mutants were made by Gibson Assembly cloning with primers listed in Supplemental Table 5. An antibiotic resistance cassette was fused to approximately 200 bp directly up- and downstream of the gene to be deleted and cloned into pBluescript. *Synechocystis* was transformed with these constructs to replace the gene with the antibiotic resistance cassette via homologous recombination. Mutants were checked via PCR for segregation (Supplemental Figure 14).

Determination of Cellular Glycogen Content and Glucose Concentration in the Growth Medium of *Synechocystis*

For full protocols, refer to Supplemental Materials and Methods. Cellular glycogen contents were determined according to a modified version of Gründel et al. (2012). Samples were taken during the exponential growth phase, 2 days upon inoculation of cultures. *Synechocystis* cells were lysed, and glycogen was precipitated and further digested to glucose with amyloglucosidase (Sigma-Aldrich, Steinheim, Germany). Glucose (derived either from glycogen or directly from the growth medium) was quantified in a coupled enzymatic test by converting it to 6-phosphogluconate with hexokinase, glucose-6-phosphate dehydrogenase, and NADP (endpoint determination). The rationale behind this test is that enzymatic conversion of glucose to 6-phosphogluconate goes hand in hand with equimolar formation of NADPH, which was quantified by a double-beam spectrophotometer (Uvikon 810; Kontron, Augsburg, Germany) at 340 nm. Glucose standards (0 mM, 0.625 mM, 1.25 mM, 2.5 mM, and 5 mM) were measured in parallel to allow quantification of glucose. Determined glucose concentrations (mM) were converted into glycogen mass (μg) by multiplying them with the lysate volume (200 μl for photoautotrophic cultures) and the molar mass ratio of glycogen to glucose (162.16/180.16). Finally, glycogen mass was converted into specific cellular glycogen content (μg/OD*ml) by dividing it by the respective OD volume.

Determination of Cellular 6-Phosphogluconate Content in *Synechocystis*

For full protocols, refer to Supplemental Materials and Methods. Samples were taken during the exponential growth phase, 2 days upon inoculation of cultures. *Synechocystis* cells were lysed and 6-phosphogluconate was quantified by converting it via 6-phosphogluconate dehydrogenase (Megazyme, Wicklow, Ireland) to ribulose-5-phosphate and CO$_2$, which goes hand in hand with equimolar formation of NADPH (endpoint determina-

tion). NADPH was quantified by a double-beam spectrophotometer (Uvikon 810; Kontron) at 340 nm. 6-Phosphogluconate standards were measured (0 mM, 0.05 mM, 0.1 mM, 0.2 mM, 0.4 mM, and 0.8 mM) to create a standard curve.

Glucose-6-Phosphate Isomerase Activity Measurements in *Synechocystis*

For full protocols, refer to Supplemental Materials and Methods. Samples were taken during the exponential growth phase, 2 days upon inoculation of cultures. In brief, glucose-6-phosphate isomerase (PGI) activity was measured in crude cell extracts photometrically in the form of NADPH turnover. Since PGI does not cause NADPH turnover itself, it was coupled to the glucose-6-phosphate dehydrogenase reaction, which causes equimolar reduction of NADP$^+$ to NADPH. Reactions were started by addition of fructose-6-phosphate and kinetics were monitored with a double-beam spectrophotometer (Uvikon 810; Kontron) for 5–10 min.

Quantification of CO$_2$ Assimilation

For full protocols, refer to Supplemental Materials and Methods. Samples were taken during the exponential growth phase, 2 days upon inoculation of cultures. In brief, CO$_2$ assimilation rates of *Synechocystis* were measured with the gas-exchange system GFS-3000 from Walz (Effeltrich, Germany). Cyanobacterial cultures were attached onto agar plates that could be inserted into the measuring device.

Determination of Photochemical Fluorescence Quenching at Photosystem II in *Synechocystis*

We tested in preliminary experiments which time span of dark incubation was efficient to arrest the CBB cycle by monitoring the quantum yield of PSII upon succeeding illumination by determining the first quantum yield after predarkening of the samples. This procedure cannot clearly discriminate between two effects: the halt of the CBB cycle and the reduction of the PQ pool via dark respiration. However, a time span of 10 min in darkness induced a significant decrease of PSII quantum yield, which did not further decrease. This indicates the achievement of (1) a steady state concerning the reduction state of the PQ pool and (2) the halt of the CBB cycle.

Until fluorescence measurements, reaction tubes with 2 ml of each *Synechocystis* genotype were illuminated with a photosynthetic photon flux density (PPFD) of 50 μmol m^{-2} s^{-1} provided by white LED lamps. A single sample was then centrifuged over 10 min (in darkness) at 3200 g and room temperature. All subsequent steps were carried out under very weak light of 0.03–0.05 μmol m^{-2} s^{-1} in order to keep the CBB cycle in an arrested state. After centrifugation, the supernatant was discarded. The pellet was gently resuspended with 75–150 μl of a new medium to adjust the OD to 20. The new medium consisted of the growth medium BG 11 without nitrate and 5 mM sodium dithionite (Merck, Darmstadt, Germany) to deplete oxygen. Subsequently, the sample was illuminated with weak blue light provided by an LED (<5 μmol m^{-2} s^{-1}) over 30 s to standardize starting conditions for all strains. Weak light was chosen to prevent the start of photosynthesis. The fluorescence signals obtained from all strains prior to and after illumination of weak blue light show that no state transition was induced ($F_{m1'}/F_{m2'}$) and that all strains were indeed in extremely similar starting conditions ($\Delta F(F_m')^{-1}$), which proves that the obtained data are comparable (Supplemental Figure 13). The subsequent measurements of chlorophyll fluorescence were performed with a PAM fluorometer (PAM 2500; Walz, Effeltrich, Germany). After 4 s the first quantum yield after predarkening of the samples was determined with a first 50-ms saturation pulse (>10 000 μmol m^{-2} s^{-1}). The illumination of the sample with red actinic light began after 40 s. Light was provided by the PAM 2500 and had a PPFD of 40 μmol m^{-2} s^{-1}. The variable fluorescence parameters F_m' and F_t were recorded within a saturation pulse protocol every 30 s over a time span of 5 min. At the end of the protocol, F_0' was determined with the internal presets of the PAM fluorometer by application of a far-red light pulse at the end of the fluorescence kinetics according to the measuring routine. The

photochemical quenching of chlorophyll fluorescence (q_P) was calculated according to the software of the fluorometer.

SUPPLEMENTAL INFORMATION

Supplemental Information is available at *Molecular Plant Online*.

AUTHOR CONTRIBUTIONS

Conceptualization, A.M., D.S., C.W., K.F., and K.G.; Methodology; A.M., L.N., D.S., and K.G.; Investigation; A.M., L.N., D.S., and K.S.; Writing – Original Draft, A.M. and K.G.; Writing – Review & Editing, A.M., L.N., D.S., K.S., C.W., K.F., and K.G.; Supervision, C.W. and K G.; Funding Acquisition; C.W., K.F., and K.G.

REFERENCES

Alagesan, S., Gaudana, S.B., Sinha, A., and Wangikar, P.P. (2013). Metabolic flux analysis of *Cyanothece* sp. ATCC 51142 under mixotrophic conditions. Photosynth. Res. **118**:191–198.

Alonso, C., and Pernthaler, J. (2006). *Roseobacter* and SAR11 dominate microbial glucose uptake in coastal North Sea waters. Environ. Microbiol. **8**:2022–2030.

Antonovsky, N., Gleizer, S., Noor, E., Zohar, Y., Herz, E., Barenholz, U., Zelcbuch, L., Amram, S., Wides, A., Tepper, N., et al. (2016). Sugar synthesis from CO_2 in *Escherichia coli*. Cell **166**:115–125.

Badger, M., and Lorimer, G. (1981). Interaction of sugar phosphates with the catalytic site of ribulose-1,5-bisphosphate carboxylase. Biochemistry **20**:2219–2225.

Bar-Even, A., Flamholz, A., Noor, E., and Milo, R. (2012). Thermodynamic constraints shape the structure of carbon fixation pathways. Biochim. Biophys. Acta **1817**:1646–1659.

Barenholz, U., Davidi, D., Reznik, E., Bar-On, Y., Antonovsky, N., Noor, E., and Milo, R. (2017). Design principles of autocatalytic cycles constrain enzyme kinetics and force low substrate saturation at flux branch points. Elife **6**:e20667.

Chen, X., Schreiber, K., Appel, J., Makowka, A., Fähnrich, B., Roettger, M., Hajirezaei, M.R., Sönnichsen, F.D., Schönheit, P., Martin, W.F., et al. (2016). The Entner-Doudoroff pathway is an overlooked glycolytic route in cyanobacteria and plants. Proc. Natl. Acad. Sci. U S A **113**:5441–5446.

Doello, S., Klotz, A., Makowka, A., Gutekunst, K., and Forchhammer, K. (2018). A specific glycogen mobilization strategy enables awakening of dormant cyanobacteria from chlorosis. Plant Physiol. **177**:594–603.

Eiler, A. (2006). Evidence for the ubiquity of mixotrophic bacteria in the upper ocean: implications and consequences. Appl. Environ. Microbiol. **72**:7431–7437.

Facchinelli, F., and Weber, A.P.M. (2011). The metabolite transporters of the plastid envelope: an update. Front. Plant Sci. **2**:50.

Flügge, U.-I., Häusler, R.E., Ludewig, F., and Gierth, M. (2011). The role of transporters in supplying energy to plant plastids. J. Exp. Bot. **62**:2381–2392.

Fuchs, G. (2011). Alternative pathways of carbon dioxide fixation: insights into the early evolution of life? Annu. Rev. Microbiol. **65**:631–658.

Gómez-Baena, G., López-Lozano, A., Gil-Martínez, J., Lucena, J.M., Diez, J., Candau, P., and García-Fernández, J.M. (2008). Glucose uptake and its effect on gene expression in prochlorococcus. PLoS One **3**:e3416.

Gründel, M., Scheunemann, R., Lockau, W., and Zilliges, Y. (2012). Impaired glycogen synthesis causes metabolic overflow reactions and affects stress responses in the cyanobacterium *Synechocystis* sp. PCC 6803. Microbiology **158**:3032–3043.

Gutekunst, K. (2018). Hypothesis on the synchronistic evolution of autotrophy and heterotrophy. Trends Biochem. Sci. **43**:402–411.

Hartmann, M., Grob, C., Tarran, G.A., Martin, A.P., Burkill, P.H., Scanlan, D.J., and Zubkov, M.V. (2012). Mixotrophic basis of Atlantic oligotrophic ecosystems. Proc. Natl. Acad. Sci. U S A **109**:5756–5760.

Howard, T.P., Metodiev, M., Lloyd, J.C., and Raines, C.A. (2008). Thioredoxin-mediated reversible dissociation of a stromal multiprotein complex in response to changes in light availability. Proc. Natl. Acad. Sci. U S A **105**:4056.

Ittekkot, V., Brockmann, U., Walter, M., and Degens, E.T. (1981). Dissolved free and combined carbohydrates during a phyto plankton bloom in the northern North Sea. Mar. Ecol. Prog. Ser. **4**:299–306.

Jansen, T., Kurian, D., Raksajit, W., York, S., Summers, M.L., and Maenpaa, P. (2010). Characterization of trophic changes and a functional oxidative pentose phosphate pathway in *Synechocystis* sp PCC 6803. Acta Physiol. Plant. **32**:511–518.

Kanno, M., Carroll, A.L., and Atsumi, S. (2017). Global metabolic rewiring for improved CO_2 fixation and chemical production in cyanobacteria. Nat. Commun. **8**:14724.

Klingner, A., Bartsch, A., Dogs, M., Wagner-Döbler, I., Jahn, D., Simon, M., Brinkhoff, T., Becker, J., and Wittmann, C. (2015). Large-scale ^{13}C flux profiling reveals conservation of the Entner-Doudoroff pathway as a glycolytic strategy among marine bacteria that use glucose. Appl. Environ. Microbiol. **81**:2408–2422.

Krüsemann, J.L., Lindner, S.N., Dempfle, M., Widmer, J., Arrivault, S., Debacker, M., He, H., Kubis, A., Chayot, R., Anissimova, M., et al. (2018). Artificial pathway emergence in central metabolism from three recursive phosphoketolase reactions. FEBS J. **285**:4367–4377.

Lam, B., and Simpson, A.J. (2008). Direct ^{1}H NMR spectroscopy of dissolved organic matter in natural waters. Analyst **133**:263–269.

Mall, A., Sobotta, J., Huber, C., Tschirner, C., Kowarschik, S., Baćnik, K., Mergelsberg, M., Boll, M., Hügler, M., Eisenreich, W., et al. (2018). Reversibility of citrate synthase allows autotrophic growth of a thermophilic bacterium. Science **359**:563.

Matsuda, F., Yoshikawa, K., Nakajima, T., Toya, Y., and Shimizu, H. (2017). Metabolic flux analysis of the *Synechocystis* sp. PCC 6803 ΔnrtABCD mutant reveals a mechanism for metabolic adaptation to nitrogen-limited conditions. Plant Cell Physiol. **58**:537–545.

Matsumura, H., Mizohata, E., Ishida, H., Kogami, A., Ueno, T., Makino, A., Inoue, T., Yokota, A., Mae, T., and Kai, Y. (2012). Crystal structure of rice rubisco and implications for activation induced by positive effectors NADPH and 6-phosphogluconate. J. Mol. Biol. **422**:75–86.

Moore, L.R. (2013). More mixotrophy in the marine microbial mix. Proc. Natl. Acad. Sci. U S A **110**:8323–8324.

Munoz-Marin, M.D., Luque, I., Zubkov, M.V., Hill, P.G., Diez, J., and Garcia-Fernandez, J.M. (2013). *Prochlorococcus* can use the

Pro1404 transporter to take up glucose at nanomolar concentrations in the Atlantic Ocean. Proc. Natl. Acad. Sci. U S A **110**:8597–8602.

Nakajima, T., Kajihata, S., Yoshikawa, K., Matsuda, F., Furusawa, C., Hirasawa, T., and Shimizu, H. (2014). Integrated metabolic flux and omics analysis of *Synechocystis* sp. PCC 6803 under mixotrophic and photoheterotrophic conditions. Plant Cell Physiol. **55**:1605–1612.

Overmann, J., and Garcia-Pichel, F. (2013). The phototrophic way of life. In The Prokaryotes: Prokaryotic Communities and Ecophysiology, E. Rosenberg, E.F. DeLong, S. Lory, E. Stackebrandt, and F. Thompson, eds. (Berlin, Heidelberg: Springer), pp. 203–257.

Owen, O.E., Kalhan, S.C., and Hanson, R.W. (2002). The key role of anaplerosis and cataplerosis for citric acid cycle function. J. Biol. Chem. **277**:30409–30412.

Papageorgiou, G.C., Tsimilli-Michael, M., and Stamatakis, K. (2007). The fast and slow kinetics of chlorophyll a fluorescence induction in plants, algae and cyanobacteria: a viewpoint. Photosynth. Res. **94**:275–290.

Saha, R., Liu, D., Hoynes-O'Connor, A., Liberton, M., Yu, J., Bhattacharyya-Pakrasi, M., Balassy, A., Zhang, F., Moon, T.S., Maranas, C.D., et al. (2016). Diurnal regulation of cellular processes in the cyanobacterium *Synechocystis* sp. strain PCC 6803: insights from transcriptomic, fluxomic, and physiological analyses. mBio **7**. https://doi.org/10.1128/mBio.00464-16.

Scanlan, D.J., Sundaram, S., Newman, J., Mann, N.H., and Carr, N.G. (1995). Characterization of a zwf mutant of *Synechococcus* sp. strain PCC 7942. J. Bacteriol. **177**:2550–2553.

Sharkey, T.D., and Weise, S.E. (2015). The glucose 6-phosphate shunt around the Calvin-Benson cycle. J. Exp. Bot. **67**:4067–4077.

Sicher, R.C. (1984). Characteristics of light-dependent inorganic carbon uptake by isolated spinach chloroplasts. Plant Physiol. **74**:962–966.

Stokes, D.M., and Walker, D.A. (1972). Photosynthesis by isolated chloroplasts. Inhibition by DL-glyceraldehyde of carbon dioxide assimilation. Biochem. J. **128**:1147–1157.

Tamoi, M., Miyazaki, T., Fukamizo, T., and Shigeoka, S. (2005). The Calvin cycle in cyanobacteria is regulated by CP12 via the NAD(H)/NADP(H) ratio under light/dark conditions. Plant J. **42**:504–513.

Teeling, H., Fuchs, B.M., Becher, D., Klockow, C., Gardebrecht, A., Bennke, C.M., Kassabgy, M., Huang, S.X., Mann, A.J., Waldmann, J., et al. (2012). Substrate-controlled succession of marine bacterioplankton populations induced by a phytoplankton bloom. Science **336**:608–611.

Wan, N., DeLorenzo, D.M., He, L., You, L., Immethun, C.M., Wang, G., Baidoo, E.E.K., Hollinshead, W., Keasling, J.D., Moon, T.S., et al. (2017). Cyanobacterial carbon metabolism: fluxome plasticity and oxygen dependence. Biotechnol. Bioeng. **114**:1593–1602.

Xiong, W., Lee, T.-C., Rommelfanger, S., Gjersing, E., Cano, M., Maness, P.-C., Ghirardi, M., and Yu, J. (2015). Phosphoketolase pathway contributes to carbon metabolism in cyanobacteria. Nat. Plants **2**:15187.

Yang, C., Hua, Q., and Shimizu, K. (2002). Metabolic flux analysis in synechocystis using isotope distribution from ^{13}C-labeled glucose. Metab. Eng. **4**:202–216.

Young, J.D., Shastri, A.A., Stephanopoulos, G., and Morgan, J.A. (2011). Mapping photoautotrophic metabolism with isotopically nonstationary (13)C flux analysis. Metab. Eng. **13**:656–665.